Differentiating Inclusion Complexes from Host Molecules by Tapping-Mode Atomic Force Microscopy

Silvia Muñoz-Botella,* M. Antonia Martín,* Benito del Castillo,* and Luis Vázquez#
*Sección Departamental de Química Analítica, Facultad de Farmacia, Universidad Complutense de Madrid, 28040 Madrid, Spain, and #Instituto de Ciencia de Materiales (CSIC), Cantoblanco, 28049 Madrid, Spain

ABSTRACT Tapping-mode atomic force microscopy imaging under different cantilever vibration amplitudes has been used to differentiate the host β-cyclodextrin nanotubes from retinal/β-cyclodextrin inclusion complex nanotubes. It was observed that both compounds were deformed differently by the applied probe force because of their different local rigidity. This change in the elasticity properties can be explained as a consequence of the inclusion process. This method shows that tapping-mode atomic force microscopy is an useful tool to map soft sample elasticity properties and to distinguish inclusion complexes from their host molecules on the basis of their different mechanical response.

INTRODUCTION

Atomic force microscopy (AFM) has been applied in biological studies since its invention (Binnig et al., 1986). Several biological systems have been successfully imaged (Yang et al., 1993; Hansma and Hoh, 1994) mainly in the contact-mode. This method has the advantage of allowing the mapping of the local elasticity properties of the sample simultaneously with the topographic imaging, which could be important in those cases where the effective stiffness of sample and cantilever are comparable (Radmacher et al., 1992). In this sense this contrast method has already proved its applicability to give information on biological soft samples (Maivald et al., 1991; Radmacher et al., 1992).

However, some experimental problems limit to some extent the range of applicability of contact-mode AFM to image soft specimens (Yang et al., 1993; Hansma and Hoh, 1994). In particular, the existence of relatively large lateral forces during constant-mode AFM imaging can lead, depending on specimen stability, to sample removing or nanocutting. This limitation has been largely reduced by AFM imaging soft samples in the so-called "tapping-mode" (Hansma et al., 1993). In this mode the probe is gently oscillating and taps the sample. In that way, the lateral forces that push aside weakly adsorbed molecules are not present and the loading forces are smaller than in contact mode (Fritz et al., 1995). Thus, soft samples can be visualized at very low forces either under ambient conditions (Hansma et al., 1993) or in liquid environments (Hansma et al., 1994; Fritz et al., 1995). However, in this mode the information regarding the elasticity properties of the sample imaged is lost. This fact is not usually as important as in contact-mode AFM because the magnitude of the applied force is much lower. In this paper we report on a simple way to differentiate relevant molecules with similar morphological features and different elasticity properties by tapping-mode AFM.

Cyclodextrin inclusion complexes (ICs) were selected as a model systems for this study considering that IC and the host molecule, β-cyclodextrin (β-CD), should exhibit the same morphology, whereas their mechanical properties change as a consequence of the inclusion process. A retinal/β-CD complex was selected as a model of CD inclusion complexes considering the chemical properties of the guest molecule and its important biological role. β-CD is a cyclic polysaccharide in which seven glucose monomers are linked, with a relatively hydrophobic cavity with the shape of a truncated cone. It is known to form ICs with many kinds of guest molecules by capturing them inside its cavity. Cyclodextrin inclusion may protect the guest molecules from their environment and several pharmaceutically interesting compounds show increased stability in the presence of cyclodextrins (Szejtli, 1982; Lerner et al., 1989). Retinal is a member of the retinoid family of compounds (Frickel, 1984). Retinoids are biologically significant compounds because of their roles as essential vitamins, in the photochemistry of vision and in cellular differentiation and proliferation. Because of their polyenic structure, retinoids are virtually insoluble in water, hydrophobic, and chemically labile, which makes their manipulation more difficult; these problems may be alleviated by cyclodextrin inclusion. The retinal molecule does not find any geometrical limitation to be included inside the β-CD cavity because of the dimensions of the β-CD (with a maximum external diameter of ≈1.5 nm and an internal diameter of ≈0.7 nm) (Le Bas et al., 1987). Also, it is well known that both, β-CD and its solid ICs can result in nanotube or filamentous structures (Tsoucaris, 1987; Li and McGown, 1994).

MATERIAL AND METHODS

Solid retinal-β-CD complexes were prepared starting from 5 ml 3×10^{-3} M hexane solution of retinal (Sigma, Saint Louis, MI). The solvent was evaporated in a round-bottomed flask, leaving a thin film of retinal in the

Received for publication 24 January 1996 and in final form 14 March 1996.

Address reprint requests to Dr. Luis Vazquez, Instituto de Ciencia de Materiales (CSIC), Cantoblanco, 28049 Madrid, Spain. Tel.: 34-1-334-9084; Fax: 34-1-372-0623; E-mail: jvara&emduam11.bitnet.

0006-3495/96/07/86/05 $2.00

bottom. 5 ml 10^{-2} M solution of β-CD in deuterium oxide were added. The reaction mixture was magnetically stirred in the dark at 20°C (thermostated bath). A fine precipitate appeared, which was collected by centrifugation and lyophilized. These complexes were redissolved in water to obtain a 10^{-6} M solution of the IC. The IC formation was verified by UV-VIS ultraviolet-visible spectrophotometry, fluorimetry, H^1- and C^{13}-NMR and infrared spectrophotometry (Muñoz Botella et al., 1996). A 20-μL drop of 10^{-6} M aqueous solution of either IC (retinal/β-CD) or the commercial β-CD (Rhône-Poulenc, Mèlle, France; and Merck, Darmstadt, Germany) was deposited on the surface of the substrate, which was a piece of freshly cleaved mica, and the water was left to evaporate to dryness before AFM imaging.

Tapping-mode AFM measurements were performed with a commercial microscope (Nanoscope III, Digital Instruments, Santa Barbara, CA). The cantilever was modulated sinusoidally at high frequencies (~300 Khz). Silicon cantilevers with ≈10 nm of a radius of curvature were employed. For our experimental equipment, it was impossible to make the measurements in a liquid environment. Thus, all the images were recorded under ambient conditions. This is justified because we were mainly interested in the solid complex. For studies in solution there are many others experimental techniques available.

The quantitation of the probe force in tapping-mode AFM is not easy (Fritz et al., 1995). However, for the experimental conditions used in this work (see the Results section), it is true that imaging at low amplitude implies lower probe force than imaging at high cantilever vibration amplitude. This was confirmed experimentally as samples harder than the cantilever, such as diamond-like films, can be imaged at low amplitudes but not at high ones (in this case the cantilever was clearly damaged). However, when soft samples were imaged at high amplitude, they were damaged or broken as was the case, in some instances, for the β-CD nanotubes studied in this work. Therefore, the cantilever vibration amplitude and the setpoint is given to describe the experimental conditions.

Imaging of the sample surface was made during the next 24 h in regions close to the border of the mark left by the drop to avoid regions of high concentration, and particular attention was paid to visualize features with an elongated shape. None of the structures shown in this work have been observed when imaging the mica surface.

RESULTS

Because of the nature of the inclusion complex, the nanotube dimensions for β-CD and IC systems should be very similar. The slight differences between them could not be resolved in our measurements because of the broadening of the measured sample features by the tip geometry (Keller, 1991). This fact was confirmed when several images of both systems were compared (Figs. 1*a*–2*a*). After averaging more than 40 β-CD and 40 IC nanotube profiles a nanotube width of ≈15 nm in both cases and an average β-CD height of 1.2 ± 0.2 nm and IC height of 0.9 ± 0.2 nm were determined. The measured width is consistent with the tip broadening effects caused by a tip with a radius of ≈10 nm (Keller, 1991) and agrees with other reported AFM width values of biological filamentous structures (Radmacher et al., 1992; Yang et al., 1993; Hansma and Hoh, 1994).

To be able to differentiate both systems, another mechanism of contrast, different from the simple topographic one, has to be used. This mechanism could be devised taking into account the different structure of both compounds. Thus, β-CD nanotubes are composed by molecules with cavities containing water molecules whereas in the IC nanotubes these cavities are filled by the ≈1.5-nm-long retinal mole-

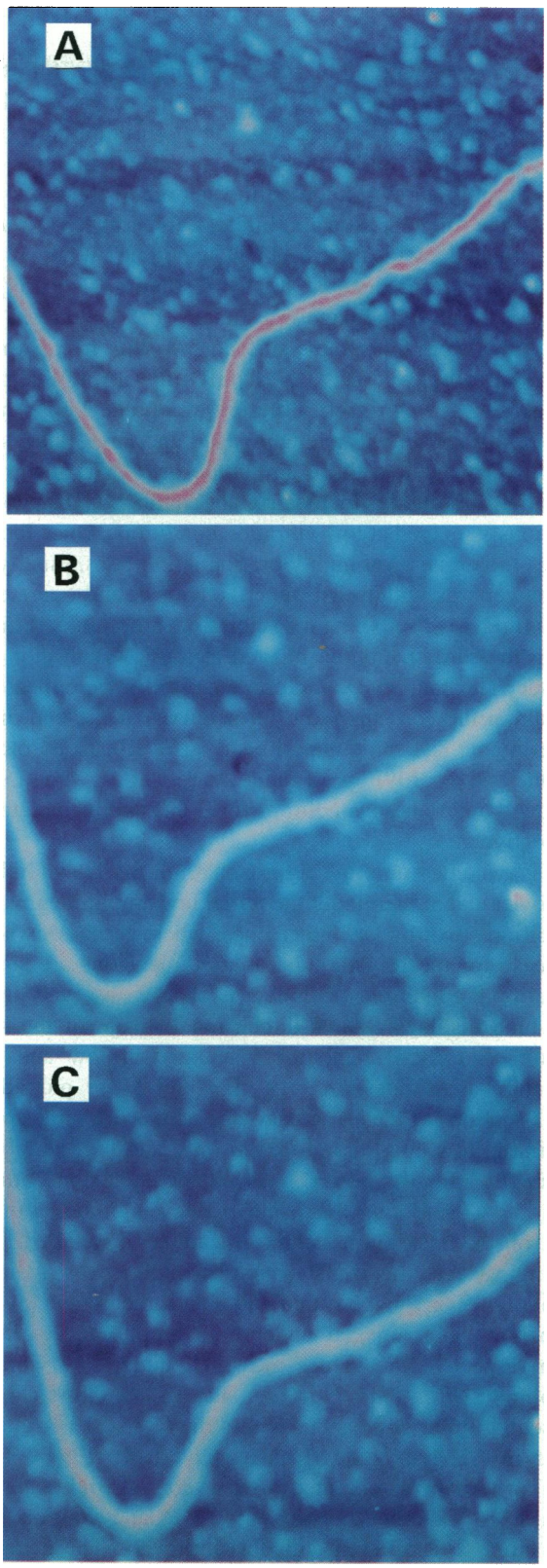

FIGURE 1 523 × 523 nm² top view tapping-mode AFM consecutive images of a β-CD nanotube imaged under: low, ≈40 nm (setpoint ≈2.5 V) (*a*), high, ≈120 nm (setpoint ≈7 V) (*b*) and again low, ≈40 nm (setpoint ≈2.5 V) (*c*) cantilever vibration amplitudes. All the images have the same vertical and color scales (the bottom is dark blue and the top is fuchsia) to help to distinguish height differences.

cules. Thus the elasticity (i.e., rigidity) of both compounds could be different.

To test the validity of these predictions the following experiment was planned: First, the cantilever was tuned at a low setpoint (≈2.5 V) and low vibration amplitude (≈40 nm). Then, the cantilever was engaged and imaging was carried out at an amplitude on the sample of the order of a 93% of the free vibration amplitude. Large images (16 μm^2) were imaged to localize a β-CD nanotube. When it was located, it was imaged at higher resolution (≈0.25 μm^2 images). After the image was taken, the cantilever was withdrawn from the sample surface and, with it ≈5 μm far from the sample, it was tuned, this time at high setpoint values (≈7 V) and high vibration amplitude (≈120 nm). Afterward, the tip was again engaged and large images (30 μm^2) were taken, with an amplitude of a 93% of the free vibration amplitude, to localize the same β-CD nanotube previously imaged at low vibration conditions. Once located it was then imaged at high vibration amplitudes. Finally the cantilever was withdrawn, tuned, engaged, and operated at the initial low setpoint and vibration amplitude settings, being the same nanotube imaged at the low vibration amplitude. The cantilever vibration amplitudes were measured by taking the corresponding force curves at the end of the experiment. The same experiment was also carried out for IC nanotubes. In Figs. 1 and 2 are shown the images obtained under these conditions for β-CD and IC nanotubes, respectively.

It is evident from both figures that the β-CD nanotube is narrower and higher under the initial low amplitude imaging conditions than under higher ones, whereas that this is not the case for the IC nanotube as its dimensions are similar under both conditions. This fact is clearly observed in Fig. 3, which displays a three-dimensional image of the same region of a β-CD nanotube visualized at low and high vibration amplitudes. In Figs. 4 *a* and 5 are plotted the cross-sections of the same nanotube across the same spot at the initial low amplitude (*dashed line*) and high amplitude (*solid line*) for the host (Fig. 4 *a*) and inclusion complex (Fig. 5). Considering the width of the nanotube as that at half of the maximum height it can be concluded, after averaging, that the β-CD nanotube experiences an increment of 40% in the measured width and a decrement of 25% in height when imaged under high amplitude conditions with respect to the values measured under low vibration amplitude (Fig. 4 *a*). However, the IC nanotube (Fig. 5) presents similar dimensions within the typical 10% range of error in AFM imaging (Hansma and Hoh, 1994). These results have been obtained after averaging more than 40 data from different nanotubes (β-CD and IC) on mica measured with different silicon cantilevers. The measured increment in the β-CD nanotube width (≈6 nm) should probably be affected by cantilever induced artifacts as the actual sample diameter is much lower (≈1.5 nm). However, the fact that the compressed β-CD nanotube is wider than the uncompressed one is consistent with a deformation without changing the quantity or density of the material of the sample. Also is important to note that, despite the possible tip artifacts, the nanotube deformation is indeed observed for the β-CD but not for the IC. It is important to note that before a high resolution imaging of the nanotube is taken, large sample areas containing it must be scanned. This implies that every nanotube scanned has previously been imaged under high vibration amplitude conditions in its entirety. Thus, it was not possible to visualize at the final low vibration amplitude, a nanotube only partially compressed (i.e. with only part of it previously imaged at high setpoint). This makes impossible to observe, on a given nanotube, the changes induced by the tip action.

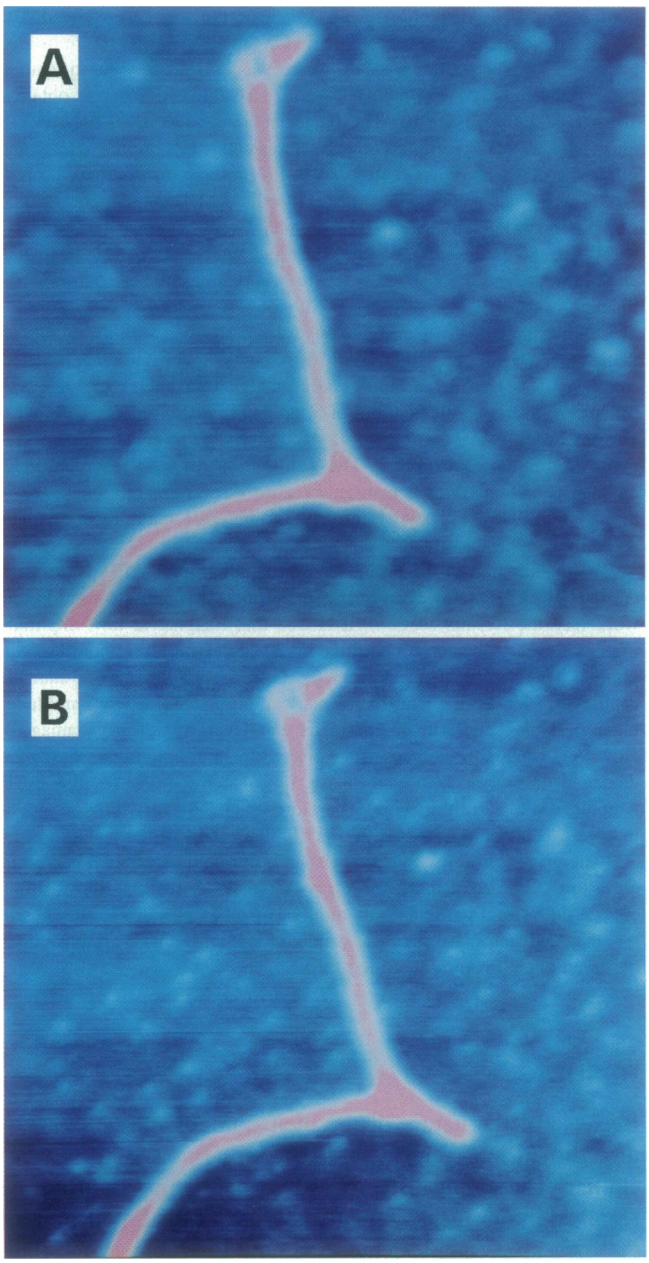

FIGURE 2 523 × 523 nm^2 top view tapping-mode AFM consecutive images of an IC nanotube imaged at: low, ≈40 nm (setpoint ≈2.5 V) (*a*), high, ≈120 nm (setpoint ≈7 V) (*b*) cantilever vibration amplitudes.

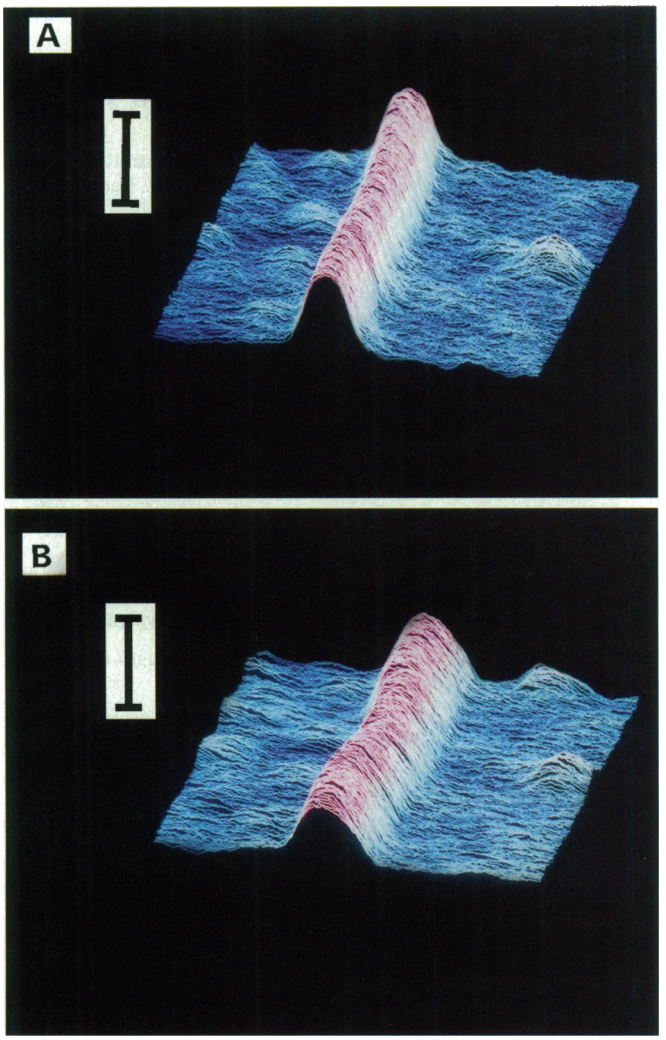

FIGURE 3 150×150 nm^2 three-dimensional images of the same region of a β-CD nanotube visualized at low, ≈40 nm (setpoint ≈2.5 V) (*a*) and high, ≈120 nm (setpoint ≈7 V) (*b*) cantilever vibration amplitudes. The bar indicates 1 nm.

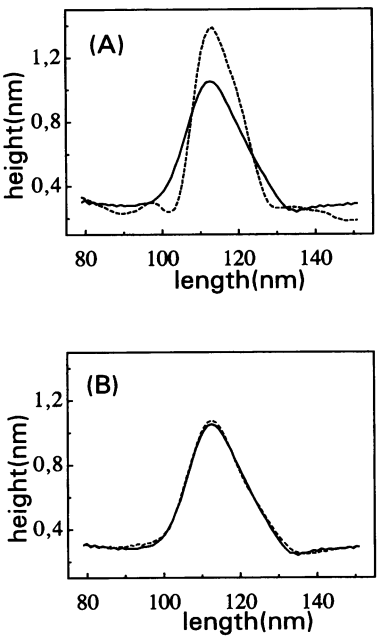

FIGURE 4 (*a*) Cross-sections of the same region of a β-CD nanotube imaged consecutively under low, ≈40 nm (setpoint ≈2.5 V), (*dashed line*) and high, ≈120 nm (setpoint ≈7 V), (*solid line*) cantilever vibration amplitudes. (*b*) Cross-sections of the same nanotube spot of Fig. 3 *a* imaged consecutively under high, ≈120 nm (setpoint ≈7 V), (*solid line*) and low, ≈40 nm (setpoint ≈2.5 V) (*dashed line*), cantilever vibration amplitudes.

The observed different mechanical response to the applied probe force for both compounds can be related to their different local rigidity as the softer compound will be more easily deformed under high probing forces. From our data the IC is more rigid than the β-CD. The IC could increase its rigidity in such a high degree as measured in this experiment because the retinal molecule, whose length is almost twice that of β-CD, must link two of the host molecules. This is supported by the 1:2 (retinal/β-CD) stoichiometry found for the inclusion complex using other techniques (Muñoz Botella, 1994).

Also, it is known that when a molecule interacts with CDs, besides geometrical constrictions that do not preclude the formation of the retinal-β-CD complex as commented above, hydrophobic interactions are the main forces involved in the inclusion of the retinal inside β-CD (Arnold et al., 1989). This is confirmed by the high association constant measured for the retinal-β-CD complex ($\log_{10} K =$ 5.99) (Muñoz Botella, 1994), which is characteristic of other β-CD inclusion complexes with hydrophobic guest-molecules such as digitoxine ($\log_{10} K = 4.23$) and progesterone ($\log_{10} K = 4.12$) (Hirayama and Uekama, 1987). So, binding of β-CD with the retinal through van der Waals interactions and hydrogen bonding is accompanied by the release of high-energy water molecules because of complex formation and the release of the strain energy in the macromolecular ring of cyclodextrin (Tan et al., 1995). Thus, IC adopts a more compact structure, in agreement with the lower IC measured height compared to that obtained for β-CD. The favored hydrophobic host cavity-guest molecule interactions lead to the high rigidity observed for the IC.

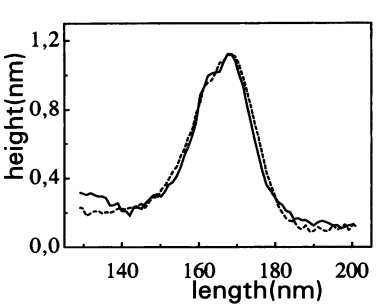

FIGURE 5 Cross-sections of the same region of an IC nanotube imaged consecutively under low, ≈40 nm (setpoint ≈2.5 V), (*dashed line*) and high, ≈120 nm (setpoint ≈7 V), (*solid line*) cantilever vibration amplitudes.

The β-CD nanotube dimensions measured when it was finally imaged again under the initial low cantilever amplitude (Fig. 1 *c*) are very close to those obtained when high amplitude was applied (Fig. 4 *b*). This means that the induced deformation is plastic rather than elastic. To understand this result it is important to consider the small length scale involved in the measurement. In a previous report on microelastic properties of biological material (a hydrated cow tibia) measured by contact-mode AFM (Tao et al., 1992) it was found that the deformation induced by the tip was elastic when large areas (≈16 μm^2) were scanned but nonelastic when small areas were sampled (≈2000 nm^2). Thus the rather local damage induced by the cantilever could explain the plastic character of the deformation observed at the nanometer level.

CONCLUSIONS

The main conclusion of this report is that the AFM operating in the tapping mode may be used as a tool to differentiate ICs from their host molecules by qualitatively mapping local mechanical properties of soft samples. For this purpose the capability of the microscope to image the same sample features at different cantilever vibration amplitudes and analyzing the eventual corresponding sample deformation is used. Thus, we observe that the β-CD nanotubes experience a nonelastic deformation when they are imaged under high cantilever vibration amplitude conditions. In contrast, the IC nanotubes have similar dimensions when they are imaged at low and high amplitudes. This experimental observation is interpreted in terms of the different local rigidity of both compounds, which causes the different mechanical response to the probe action. The IC nanotube higher rigidity is explained as a consequence of the formation of the inclusion complex, whereas the plastic character of the deformation observed for the β-CD nanotube is understood as a consequence of the local nature of the damage caused by the probe action. Also, it can be concluded that for filamentous biological samples it is safer to give as the filament width that obtained at low vibration amplitudes. Finally, one further field of application may be that of polymer compounds where ions or anions are incorporated inside the polymer structure (Vork et al., 1990) as well as other compounds able to form inclusion complexes like ciclophanes. This incorporation could change the elasticity properties that would be mapped by AFM.

We acknowledge helpful discussions with Dr. R. Salvarezza, Dr. J.A. Martin-Gago, and Dr. R. García. We are also indebted to Instrumat Técnicas de Medición S.A. (Barcelona, Spain) and Digital Instruments (Santa Barbara, CA, U.S.A.) for their technical support.

REFERENCES

Arnold, E. N., T. S. Lillie, and T. E. Beesley. 1989. Molecular modeling of cyclodextrin-guest molecule interactions. *J. Liq. Chromatogr.* 12: 337–343.

Binnig, G., C. F. Quate, and C. Gerber. 1986. Atomic force microscope. *Phys. Rev. Lett.* 56:930–933.

Frickel, F. 1984. Chemistry and physical properties of retinoids. *In* The Retinoids, Vol. 1. M. B. Sporn, A. B. Roberts, and D. S. Goodman, editors. Academic Press, Orlando, FL. 8–145.

Fritz, M., M. Radmacher, J. P. Cleveland, M. W. Allersma, R. J. Stewart, R. Gieselmann, P. Janmey, C. F. Schmidt, and P. K. Hansma. 1995. Imaging globular and filamentous proteins in physiological buffer solutions with tapping mode atomic force microscopy. *Langmuir.* 11: 3529–3535.

Hansma, P. K., J. P. Cleveland, M. Radmacher, D. A. Walters, P. E. Hillner, M. Bezanilla, M. Fritz, D. Vie, H. G. Hansma, C. B. Prater, J. Massie, L. Fukunaga, G. Gurley, and V. Elings. 1994. Tapping mode atomic force microscopy in liquids. *Appl. Phys. Lett.* 64:1738–1740.

Hansma, H. G., and J. Hoh. 1994. Biomolecular imaging with the atomic force microscope. *J. Ann. Rev. Biophys. Biomol. Struct.* 23:115–139.

Hansma, H. G., R. L. Sinsheimer, J. Groppe, T. C. Bruice, V. Elings, G. Gurley, M. Bezanilla, I. A. Mastrangelo, P. V. C. Hough, and P. K. Hansma. 1993. Recent advances in atomic force microscopy of DNA. *Scanning.* 15:296–299.

Hirayama, F., and K. Uekama. 1987. Methods on investigating and preparing inclusion compounds. *In* Cyclodextrins and Their Industrials Uses. D. Duchêne, editor. Editions de Santé, Paris. 142–144.

Keller, D. 1991. Reconstruction of STM and AFM images distorted by finite-size tips. *Surf. Sci.* 253:353–364.

Le Bas, G., and N. Rysanek. 1987. Structural aspects of cyclodextrins. *In* Cyclodextrins and Their Industrials Uses. D. Duchêne, editor. Editions de Santé, Paris. 107–130.

Lerner, D. A., B. del Castillo, and S. Muñoz Botella. 1989. Room temperature luminescence of a retinal complex of cyclodextrin. *Anal. Chim. Acta.* 227:297–301.

Li, G., and L. B. McGown. 1994. Molecular nanotube aggregates of β- and γ-cyclodextrins linked by diphenylhexatrienes. *Science.* 264:249–251.

Maivald, P. H., H. J. Butt, S. A. C. Gould, C. B. Prater, B. Drake, J. A. Gurley, V. B. Elings, and P. K. Hansma. 1991. Using force modulation to image surface elasticities with the atomic force microscope. *Nanotechnology.* 2:103–106.

Muñoz Botella, S. 1994. Formación de complejos de inclusión entre retinoides y ciclodextrinas: características, propiedades y ventajas analíticas. Ph. D. Thesis, Universidad Complutense de Madrid, Madrid. 319–341.

Muñoz Botella, S., M. A. Martín, B. del Castillo, J. C. Menéndez, L. Vázquez, and D. A. Lerner. 1996. Synthesis, isolation and characterization of a retinal/β-cyclodextrin complex. *J. Pharmacol. Biomed. Anal.* In press.

Radmacher, M., R. W. Tillmann, M. Fritz, and H. E. Gaub. 1992. From molecules to cells: imaging soft samples with the atomic force microscope. *Science.* 257:1900–1905.

Szejtli, J. 1982. Cyclodextrins and Their Inclusion Complexes. Akademiai Kiado, Budapest.

Tao, N. J., S. M. Lindsay, and S. Lees. 1992. Measuring the microelastic properties of biological material. *Biophys. J.* 63:1165–1169.

Tan, Z. J., X. X. Zhu, and G. R. Brown. 1995. Formation of inclusion complexes of cyclodextrins with bile salt anions as determined by NMR titration studies. *Langmuir.* 10:1034–1039.

Tsoucaris, G. 1987. Clathrates and solid inclusion compounds. *In* Cyclodextrins and Their Industrials Uses. D. Duchêne, editor. Editions de Santé, Paris. 19–76.

Vork, F. T. A., B. C. A. M. Schuermans, and E. Barendrecht. 1990. Influence of inserted anions on the properties of polypyrrole. *Electrochim. Acta.* 35:567–575.

Yang, J., L. K. Tamm, A. P. Somlyo, and Z. Shao. 1993. Promises and problems of biological atomic force microscopy. *J. Microscopy.* 169: 183–198.